Optics and Photonics Journal, 2023, 13, 63-78
https://www.scirp.org/journal/opj
ISSN Online: 2160-889X
ISSN Print: 2160-8881

Detection of Rice Yellow Mottle at the Asymptomatic Stage by Hyperspectral Fluorescence and Reflectance Spectroscopies

Amara Kamate[1], Penetjiligué Adama Soro[1], Emma Georgina Zoro-Diama[1], Kedro Sidiki Diomandé[2], Adjo Viviane Adohi-Krou[1]

[1]Laboratoire des Sciences de la Matière, de l'Environnement et de l'Energie Solaire (LASMES), Université Félix Houphouët-Boigny, Abidjan, Côte d'Ivoire
[2]Centre National de Recherche Agronomique (CNRA), Adiopodoumé, Côte d'Ivoire
Email: gina_zoro@yahoo.fr

How to cite this paper: Kamate, A., Soro, P.A., Zoro-Diama, E.G., Diomandé, K.S., and Adohi-Krou, A.V. (2023) Detection of Rice Yellow Mottle at the Asymptomatic Stage by Hyperspectral Fluorescence and Reflectance Spectroscopies. *Optics and Photonics Journal*, **13**, 63-78.
https://doi.org/10.4236/opj.2023.134005

Received: April 13, 2023
Accepted: April 27, 2023
Published: April 30, 2023

Abstract

Rice yellow mottle is considered the most destructive disease threatening rice production in Africa. Early detection of this infection in rice is essential to limit its expansion and proliferation. However, there is no research devoted to the spectral detection of rice yellow mottle virus (RYMV) infection, especially in the asymptomatic or early stages. This work proposes the use of hyperspectral fluorescence and reflectance data at leaf level for the detection of this disease in asymptomatic stages. A greenhouse experiment was therefore conducted to collect hyperspectral fluorescence and reflectance data at different stages of infection. These data allowed to calculate nine vegetation indices: one from fluorescence spectra and eight from reflectance spectra. A t-test made it possible to identify, from the second day after infection, four relevant reflectance vegetation indices to discriminate healthy leaves from those infected: these are Photochemical Reflectance Index (PRI), Transformed Chlorophyll Absorption in Reflectance Index (TCARI), Structure Intensive Pigment Index (SIPI) and Simple Ratio Pigment Index (SRPI). The fluorescence index was less sensitive in detecting infection. The four significant vegetation indices for the detection of RYMV were then used to build and evaluate models for discriminating plants according to their health status by the supervised classification of support vector machine (SVM) at different stages of infection. The maximum overall accuracy is 92.5% six days after inoculation (6 DAI). The sixth day after inoculation would be the adequate day to detect RYMV. This plants discrimination was validated by the mean reflectance spectra and by the histograms showing the differences between the average reflectance vegetation indices values of the two types of plants. Our results demonstrate the feasibility of differentiating RYMV-infected samples.

They suggest that support vector machine learning models could be developed to diagnose RYMV-infected plants based on vegetation indices derived from spectral profiles at early stages of disease development.

Keywords

Rice Yellow Mottle Virus, Fluorescence Spectra, Reflectance Spectra, Vegetation Indices, SVM Classification, Savitzky Golay Filtering

1. Introduction

A staple food for the world's population, rice (*oryza sativa*) contributes to the food security of many countries, especially the developing countries. Along with wheat and maize, rice is one of the three most widely cultivated cereals in the world. According to the Centre de coopération Internationale en Recherche Agronomique pour le Développement (CIRAD), in 2021, rice global production reached 525 million tons. Almost 90% of this production is cultivated and consumed in Asia [1].

In Côte d'Ivoire, rice cultivation represents 6% to 8% of food production and 57.06% of areas cultivated with cereals [2]. Local production does not cover national needs. The country therefore imports a large amount of rice each year to meet the food needs of its population. The low rice production in Côte d'Ivoire is partly due to abiotic and biotic factors, the most important of which is the Rice Yellow Mottle Virus (RYMV), which is confined only to Africa. The pathogen, RYMV can be transmitted mechanically by beetles, mainly from the *Chrysomelidae* family and other insects such as Conocephalus spp [3] [4] [5] [6]. Other routes of transmission exist through frictions between healthy plants and diseased plants under the action of wind or people [7]. The disease is manifested by the appearance of yellow streaks on the leaf surface, followed by total discoloration and then leaf necrosis. Plants experience reduced growth with poor panicle exsertion and often become sterile; leading to high yield losses [8] [9]. Harvest losses due to this rice virus vary from 20% to 100% depending on the rice variety, the virus strain, the vegetative stage of the plant and the environment [10] [11] [12]. Visual inspection is the commonly used method to monitor and detect rice yellow mottle in the field. But this method is tedious and subjective. Other diagnostic techniques such as immunoenzymatic detection, polymerase chain reaction and recombinase polymerase amplification (RPA) are also used [13]. But they are time-consuming, destructive and require high level of technology. Spectral, multispectral and hyperspectral remote sensing techniques, which are non-destructive and rapid, have proven to be very useful for crop diseases detection.

Thus, Fernandez *et al.* [14] successfully detected early symptoms of potato late blight at leaf and canopy levels on hyperspectral reflectance data using support vector machines (SVM). The results indicate that the potato disease can be identified at least three days before the onset of symptoms. SVM has also been used by Moshou *et al.* [15] to show that the fusion of fluorescence and reflectance data collected on wheat leaves makes it possible to optimize the simultaneous detection of biotic stress due to the fungus *Septotria tritici* and abiotic stress related to water deficiency. Hermann *et al.* [16] established models to identify non-visual foliage symptoms induced by *Fusarium virguliforme* in soybean using Partial Least Squares Discriminant Analysis (PLSDA) of canopy reflectance data. A methodology to detect leaves affected by rice pyriculariosis at different stages of plant development was developed by Tian *et al.* [17]. They showed that the combination of two to four spectral features selected by the Machine Learning based Sequential Floating Forward Selection (ML-SFFS) algorithm was sufficient to identify infected leaves with a classification accuracy greater than 80% for early stages of the infection.

However, there is no research devoted to the spectral detection of rice yellow mottle virus. This disease, located exclusively in Africa, is the most destructive because it causes a sharp drop in rice production [18] and threatens food security on the continent. In this present work, we combined visible/near infrared (Vis/NIR) hyperspectral information of chlorophyll fluorescence and reflectance to detect, at an asymptomatic stage, yellow mottle on rice leaves.

The plant material and the experimental setup for acquisition of fluorescence and reflectance hyperspectral data are presented. Then, the identification of relevant vegetation indices using the t-test is performed. Finally, performance evaluation of these vegetation indices relevant to RYMV detection using SVM classification is explained.

2. Materials and Methods

2.1. Plant Material and Experimental Plan

The plant material used in this study is the Bouaké 189 rice variety. The seeds of this variety were provided by the Centre National de Recherche Agronomique (CNRA) in Côte d'Ivoire. The experiment was conducted in a greenhouse at the scientific and innovation center of the Félix Houphouët-Boigny University, located at altitude 05˚21'36.1"N and longitude 03˚54'08.6"W. The experimental plantation consisted of three repetitions with two treatments (healthy plants and infected plants).

Five rice grains of the Bouaké 189 variety were sown at a depth of 2 cm in 5 kg of soil initially placed in plastic cultivation pots with a capacity of 5 L, and 24 cm in diameter at the opening. It should be noted that the soil used contained all the nutrients necessary for the proper development of the rice plants. Seven days after sowing, two plants per pot were retained. During the experimental period, the average temperature in the greenhouse was 27.8˚C and the humidity was 82.5%.

2.2. Inoculum Preparation and Inoculation

Samples of rice leaves showing the characteristic symptoms of rice yellow mottle were ground at the rate of 10 g of leaves per 100 ml of distilled water in a mortar previously cleaned with alcohol. Carborundum (600 mesh, 5 mg/ml) was added to the raw extract to promote viral infiltration [19]. Twenty-one days after sowing, half of the rice plants were mechanically inoculated by hand friction. This inoculation consisted of gently rubbing from bottom to top, the rice plants leaves using fingers dipped in the inoculum. The leaves of healthy plants were rubbed in the same way but with a mixture of distilled water and carborundum. To avoid possible contamination of healthy plants, these were separated from infected plants. All plants were regularly watered for the duration of the experiment to avoid water stress.

2.3. Experimental Setup

Spectral data were collected *in vivo* and *in situ* using the USB 4000 spectrometer from Ocean Optics company. This spectrometer allows the acquisition of spectral data in the visible and near infrared regions (350 nm to 1100 nm) with a 0.22 nm sampling pitch. Fluorescence and reflectance spectra of rice leaves were acquired from the leaves using a bifurcated optical fiber. The spectral response of the leaves was obtained from the average of three measurements. In fluorescence mode, the samples were excited by a blue LED (LS-450) emitting at 450 nm [20] [21]. In reflectance mode, the samples were excited by a halogen lamp. Note that reflectance measurements require the prior use of a white lambertian surface (reference surface). The acquisition, storage and processing of the collected spectral data were carried out using a laptop computer. **Figure 1** illustrates the experimental setup of the two measurement modes.

2.4. Vegetation Indices

Vegetation indices were used to correlate fluorescence and reflectance values to the physicochemical characteristics of plants. Most of these vegetation indices

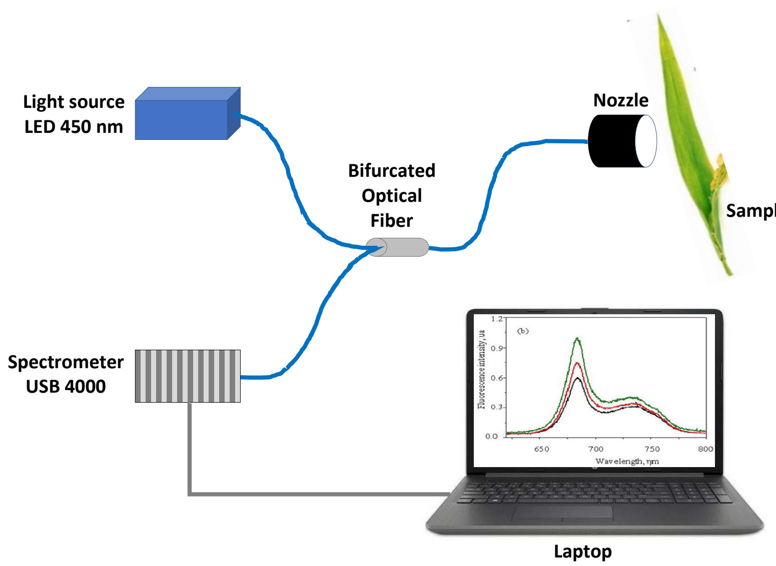

(a)

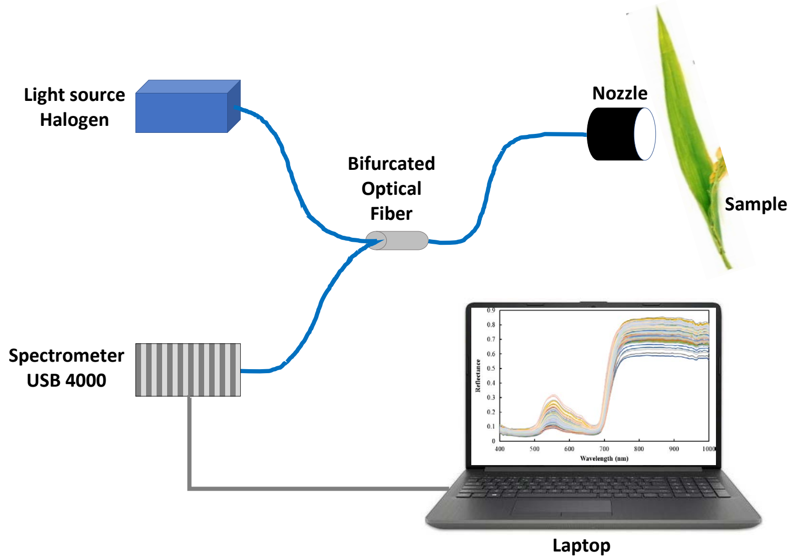

(b)

Figure 1. Experimental setup: (a) in fluorescence mode; (b) in reflectance mode.

are obtained by arithmetic combinations of spectral bands. Considering the spectral band of our apparatus, we selected nine (9) vegetation indices as potential candidates to detect rice yellow mottle: one (1) fluorescence index and eight (8) reflectance indices. These were then computed using Matlab R2017a software. Table 1 presents for each selected vegetation index, the calculation formula based on the reflectance or fluorescence values in the visible and near infrared.

2.5. Hyperspectral Data Analysis

All hyperspectral data were processed using Matlab R2017a software. The spectra collected from the leaves of healthy and infected plants were first cropped in the spectral ranges: 640 nm to 800 nm for the chlorophyll fluorescence spectra and 400 nm to 1000 nm for the reflectance spectra. These different spectra were subjected to Savitzky Golay filtering [31] using the second-order polynomial and a window size of 33 data points to reduce instrumental noise. In addition to filtering, fluorescence spectra were normalized while reflectance spectra underwent a multiplicative scattering correction [32]. For each measurement day, the average of the pretreated spectra of the two types of samples (healthy plants and infected plants) was determined. Then, the mean spectra were plotted on the same graph to observe the spectral variations as a function of the duration of the infection.

The data were acquired on 120 leaves for a period between two and twelve Days After virus Inoculation (2 DAI and 12 DAI). Over this measurement period, the selected vegetation indices were calculated. We then looked for significant differences between healthy and infected plants as a function of the duration of infection, using the t-test on the indices.

Table 1. Vegetation indices used to detect rice yellow mottle.

Vegetation indices	Equations	References
Fluorescence Ratio Index (FRI)	$\text{FRI} = \frac{F_{685}}{F_{735}}$	Méthy *et al.* (1991) [22]
Fluorescence Reflectance Index 1 (FRI_1)	$\text{FRI}_1 = \frac{R_{690}}{R_{600}}$	Dobrowski *et al.* (2005) [23] Sun *et al.* (2008) [24]
Fluorescence Reflectance Index 2 (FRI_2)	$\text{FRI}_2 = \frac{R_{740}}{R_{800}}$	Dobrowski *et al.* (2005) [23] Sun *et al.* (2008) [24]
Photochemical Reflectance Index (PRI)	$\text{PRI} = \frac{R_{531} - R_{570}}{R_{531} + R_{570}}$	Gamon *et al.* (1992) [25]
Normalized Difference vegetation index (NDVI)	$\text{NDVI} = \frac{R_{800} - R_{670}}{R_{800} + R_{670}}$	Rouse *et al.* (1974) [26]
Structure Intensive Pigment Index (SIPI)	$\text{SIPI} = \frac{R_{800} - R_{445}}{R_{800} - R_{680}}$	Penuelas *et al.* (1995) [27]
Simple Ratio Pigment Index (SRPI)	$\text{SRPI} = \frac{R_{430}}{R_{680}}$	Penuelas *et al.* (1994) [28]
Red Edge Inflation Point (REIP)	$\text{REIP} = 700 + 40 \times \frac{0.5(R_{670} + R_{780}) - R_{700}}{R_{740} - R_{700}}$	Guyot *et al.* (1988) [29]
Transformed Chlorophyll Absorption in Reflectance Index (TCARI)	$\text{TCARI} = \frac{3 \times \left[(R_{700} - R_{670}) - 0.2 \times (R_{700} - R_{550}) \times \left(\frac{R_{700}}{R_{670}} \right) \right]}{(1 + 0.16) \times \frac{R_{800} - R_{670}}{R_{800 + R_{670} + 0.16}}}$	Haboudane *et al.* (2002) [30]

Vegetation indices relevant to the detection of rice yellow mottle were used to perform support vector machine discriminant analysis (SVM-DA) to build discrimination models of healthy and infected plants. The SVM-DA technique is a robust machine learning algorithm developed by Cortes and Vapnik (1995) [33] to classify data into two groups. The Gaussian function, a core function used for non-linear problems, was employed in the study to reduce the computational complexity of the calibration procedure and improve the prediction results. The parameters of this function (kernel width and cost factor) are optimally selected based on minimizing the misclassification error. Our database was randomly divided into two subsets: a training subset and a test subset comprising respectively 2/3 and 1/3 of the 120 vegetation indices. The distribution of data is shown in Table 2.

According to Ballabio *et al.* [34] and Shrestha *et al.* [35], the performance of the SVM model can be evaluated by the sensitivity (SN), the specificity (SP) and the Accuracy. These parameters are defined by Equations (1) to (3).

$$\text{SN} = \frac{TP}{TP + FN} \tag{1}$$

$$\text{SP} = \frac{TN}{TN + FP} \tag{2}$$

$$\text{Accuracy} = \frac{\text{correctly classified samples}}{\text{Total samples}} \quad (3)$$

where TP is the number of true positive, TN is the number of true negative, FP is the number of false positive, FN is the number of false negative. Sensitivity is the ability of the model to correctly identify a group of samples, whereas specificity is the ability to reject samples from other groups.

The data analysis process is summarized by the flowchart in Figure 2.

3. Results and Discussion

At the end of the experiment (12 DAI), the yellow mottle are now visible on infected rice leaves. Figure 3 shows photographs of healthy and the infected leaves.

Table 2. Distribution of samples used for classification.

Database	Subset	Healthy leaves	Infected leaves	Total
Fluorescence and Reflectance indices	Train	80	80	160
	Test	40	40	80

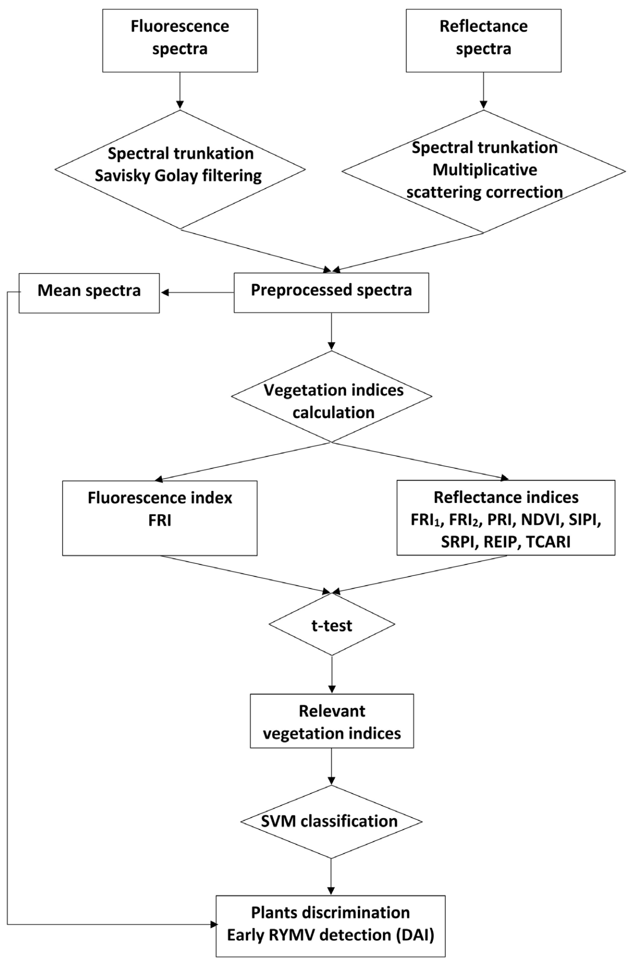

Figure 2. Rice yellow mottle detection process.

3.1. Average Fluorescence Spectra

The mean fluorescence spectral signatures of the healthy leaves and the rice yellow mottle virus infected leaves are presented as a function of the number of days after inoculation in **Figure 4**. The mean fluorescence spectra of both samples'

(a) (b)

Figure 3. Photographs of healthy and infected leaves at 12 DAI: (a) healthy leaf; (b) infected leaf.

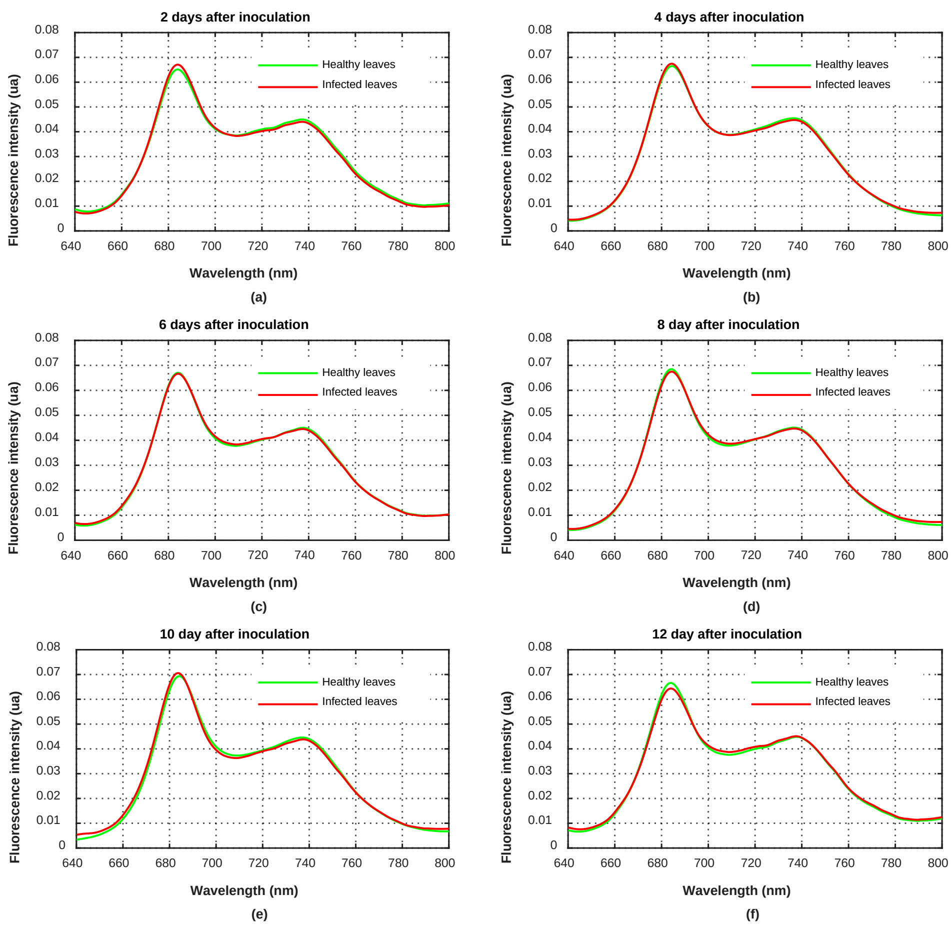

Figure 4. Mean leaf fluorescence spectra of healthy plants and rice yellow mottle infected plants as a function of the number of days after inoculation (a)-(f).

types correspond to an average value of 120 spectra. The shape of the fluorescence spectra of healthy and infected leaves are similar. Fluorescence emission peaks in the red and near infrared are evident on the spectra. However, slight differences between the two spectra are observed around the fluorescence emission peaks of chlorophyll *a* in the red at 685 nm and in the near infrared at 735 nm, demonstrating that the RYMV influences the plant spectral characteristics.

3.2. Mean Reflectance Spectra

The mean reflectance spectra of healthy and infected leaves as a function of the number of days after inoculation are presented in **Figure 5**. They correspond to the average value of 120 leaves spectra of both samples' types. The appearance of the mean reflectance spectra of healthy and infected leaves is similar. However, there are differences between the reflectance values of both samples' types at green, red and near-infrared wavelengths. Indeed, infected plants show a higher reflectance than healthy plants for these wavelengths. The effects of RYMV on the leaf reflectance spectrum are detected in the visible and near-infrared regions (550 nm to 1000 nm).

The mentioned wavelengths are associated with chlorophyll content, photosynthetic efficiency and internal leaf structure.

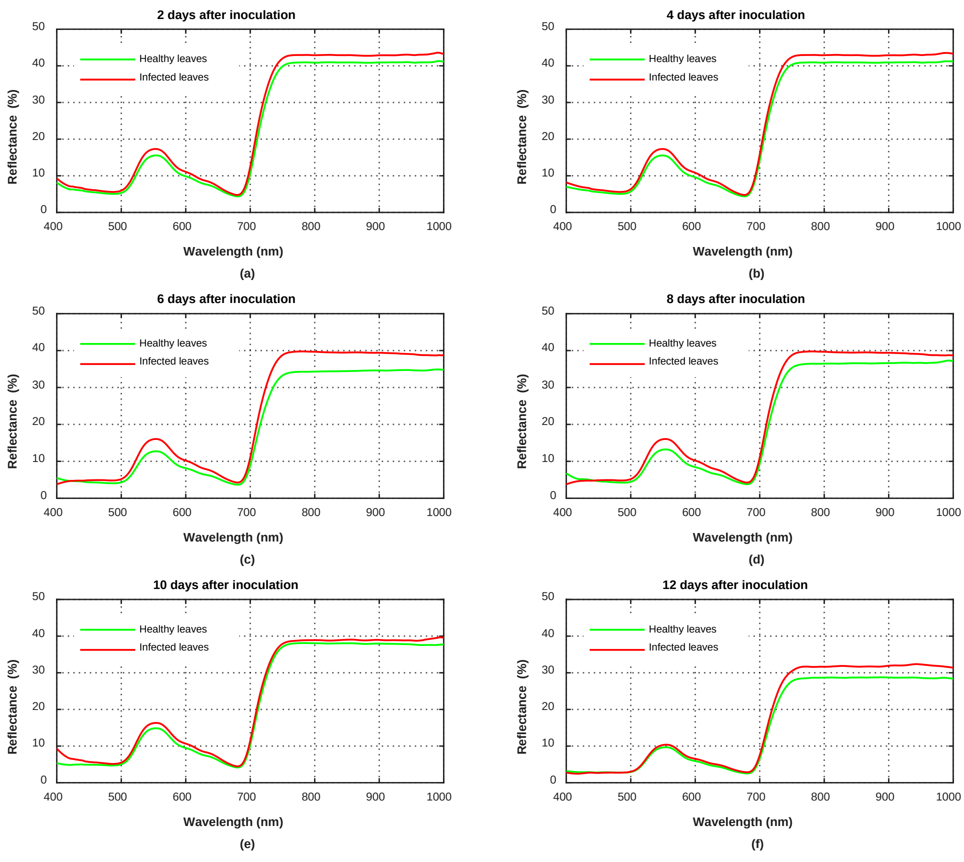

Figure 5. Mean reflectance spectra of healthy and infected with rice yellow mottle leaves plants as a function of the number of days after inoculation (a)-(f).

Observation of the graphs in Figure 4 and Figure 5 allows to deduce that the mean reflectance spectra discriminate healthy plants from the plants infected by yellow rice mottle, unlike the mean fluorescence spectra.

3.3. Temporal Sensitivity of Selected Vegetation Indices

Significant differences in mean values of healthy and infected plant vegetation indices are presented in Table 3.

Table 3. Significant differences between mean values of healthy and infected plant vegetation indices.

Indices	Treatments	2 DAI	4 DAI	6 DAI	8 DAI	10 DAI
FRI	Healthy	1.458	1.508	1.545	1.566	1.461
	Infected	1.469	1.512	1.504	1.627	1.537
	p value	ns	ns	***	***	***
FRI_1	Healthy	0.757	0.763	0.762	0.760	0.775
	Infected	0.748	0.755	0.712	0.788	0.760
	p value	ns	ns	***	***	**
FRI_2	Healthy	0.937	0.950	0.941	0.943	0.943
	Infected	0.937	0.952	0.953	0.963	0.948
	p value	ns	ns	***	***	***
PRI	Healthy	0.029	0.028	0.037	0.031	0.030
	Infected	0.017	0.030	0.059	0.025	0.027
	p value	***	***	***	***	***
NDVI	Healthy	0.832	0.800	0.812	0.816	0.796
	Infected	0.830	0.799	0.802	0.803	0.786
	p value	ns	ns	ns	***	**
OSAVI	Healthy	0.960	0.925	0.939	0.943	0.920
	Infected	0.958	0.923	0.927	0.928	0.909
	p value	ns	ns	ns	***	**
TCARI	Healthy	21.486	29.159	30.999	31.838	33.131
	Infected	23.103	31.52	42.727	34.247	37.219
	p value	***	***	**	***	***
SIPI	Healthy	0.994	0.979	0.972	0.984	0.983
	Infected	1.011	0.984	0.929	0.989	0.971
	p value	***	***	***	***	***
SRPI	Healthy	1.105	1.278	1.305	1.223	1.150
	Infected	0.909	1.183	3.143	1.142	1.327
	p value	***	***	*	***	***
REIP	Healthy	714.758	713.857	714.825	714.164	713.176
	Infected	714.414	713.568	714.451	712.878	711.914
	p value	ns	ns	ns	***	***

* = Significant at 0.05; ** = Significant at 0.01; *** = Significant at 0.001; ns = Non Significatif.

The t-test analysis of vegetation indices reveals that there is a significant difference between healthy and infected plants. Indeed, from the second day after inoculation (2 DAI), four reflectance vegetation indices (PRI, TCARI, SIPI, SRPI) indicate a significant difference in their mean values for both types of plants. The difference between the values of the vegetation indices FRI, FRI_1 and FRI_2 of the healthy and infected plants is significant from the sixth day after inoculation. From 8 DAI, there is a significant difference between the average values of all the vegetation indices of healthy and infected plants. All these results show that the calculated vegetation indices allow to discriminate healthy plants from infected ones at the asymptomatic stage. PRI, SIPI, SRPI and TCARI proved to be the best vegetation indices for this discrimination. These indices were calculated from the reflectance data. This corroborates the observation made from the mean reflectance spectra.

For each of the relevant vegetation indices (PRI, SIPI, SRPI and TCARI) for the rice yellow mottle detection, the difference between their mean values of healthy leaves and infected leaves is calculated. The results are given for each day of measurements as histograms in Figure 6.

Figure 6 clearly shows that the greatest difference between the mean values of the vegetation indices of the infected plants and healthy plants is obtained at 6 DAI for all the four relevant indices. So, at this date there would have a higher discrimination between the two groups of plants. The infected plants felt more the effects of the infection although these are not yet visible on the leaves. This result is consistent with the mean reflectance spectra in Figure 5(c) which are well separated on the sixth day after inoculation.

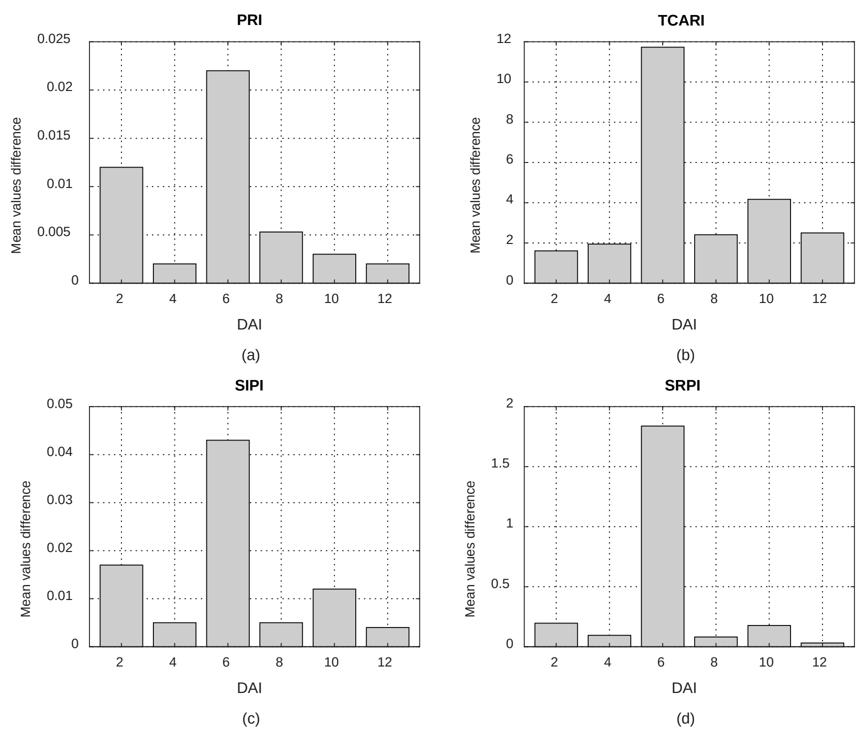

Figure 6. Differences mean values of vegetation indices of healthy and infected plants.

3.4. Detection of RYMV Infection Using the SVM Classification Technique

After determining the best vegetation indices for the detection of rice yellow mottle, SVM discriminant analysis models were built to test whether these indices can be used to classify plants according to their status (healthy or infected leaves) depending on the time after inoculation. Detailed performances of the SVM models are presented as a function of the number of days after inoculation in **Table 4**.

The overall accuracy of the SVM tests is 71.25% two days after inoculation (**Table 4**). This low classification rate corresponds to the slight difference between the reflectance spectra in **Figure 5(a)**. The overall classification accuracy increased to reach the maximum value of 92.50% six days after inoculation. This last result confirms those given by **Figure 5(c)** and **Figure 6**. Therefore, the sixth day after inoculation (6 DAI) would be the ideal day to perform measurements to detect the rice plant infection by RYMV.

Due to the lack of research dedicated to the spectral detection of rice yellow mottle, we compared our results to those obtained by research teams using spectroscopic disease detection methods for other crops. In the context of our study, the highest classification accuracy (92.50%) was achieved at 6 DAI when the disease was well established. This accuracy was of the same order of magnitude as that (93.00%) obtained at 4 DAI by Römer *et al.* [36] who applied an SVM classifier to fluorescence data induced by ultraviolet radiation. These data were acquired between 370 and 800 nm on healthy and *Puccinia triticia* infected winter wheat leaves. However, the maximum classification accuracy that we obtained is higher than that (91.11%) obtained by Fernández *et al.* [14] at the leaf scale for 4 DAI and 5 DAI. This team of researchers applied the PLS-DA method to reflectance spectra (400 nm - 900 nm) to discriminate healthy potato plants from plants infected with late blight.

Table 4. SVM-DA test prediction results according DAI.

Number of days after inoculation	Dataset	Sensitivity (%)	Specificity (%)	Accuracy (%)
2 DAI	Train	100	100	100
	Test	67.35	77.42	71.25
4 DAI	Train	100	100	100
	Test	95.45	67.24	75
6 DAI	Train	100	100	100
	Test	100	86.96	92.50
8 DAI	Train	100	100	100
	Test	76.92	100	85.00
10 DAI	Train	100	100	100
	Test	100	83.34	90
12 DAI	Train	100	100	100
	Test	75.51	90.32	81.25

4. Conclusions

In this study, we analyzed the spectral detection of RYMV infection at foliar level. Rice plants of the Bouaké 189 variety were grown in a greenhouse. Fluorescence and reflectance spectra of the leaves were acquired using a portable USB 4000 spectrometer for a period of 2 to 12 DAI. Applying the t-test to the vegetation indices showed that there is a significant difference between healthy and infected plants. In addition, the reflectance indices PRI, TCARI, SIPI and SRPI have proven to be the best for this discrimination because they allow detection of the disease from the second day after infection. The fluorescence index is less sensitive to the infection detection.

Support vector machine discriminant analysis was then applied to these four relevant vegetation indices to differentiate plants according to their health status. The overall classification accuracy on the second day after inoculation (2 DAI) was 71.25% and reached a maximum value of 92.50% six days after inoculation. This better discrimination was validated by the mean reflectance spectra and the differences between the average values of the vegetation indices. This shows that the sixth day after inoculation (6 DAI) would be the appropriate day to carry out the measurements for the rice yellow mottle detection. The low detection performance of rice yellow mottle from fluorescence data could be related to the excitation source. Excitation of samples by the ultraviolet radiation could allow better detection of this rice viral disease.

Supervised SVM classification of reflectance vegetation indices holds promise for early-stage disease diagnosis. As Côte d'Ivoire is the world's leading cocoa producer, early detection of swollen shot, a viral disease of cocoa, could help fight against this scourge and improve the cocoa farmers income.

Acknowledgements

We would like to thank the Programme d'Appui Stratégique à la Recherche Scientifique (PASRES) for funding our study and the Centre National de Recherche Agronomique (CNRA) for its scientific collaboration.

Conflicts of Interest

The authors declare no conflicts of interest regarding the publication of this paper.

References

[1] The French Agricultural Research Centre for International Development (2022) Synthèse de la feuille de route riz: Vers une riziculture durable [2023-2033]. https://www.cirad.fr/view_pdf/7638

[2] Tano, J.S.C. and Koné, A. (2021) Analyse des effets de distorsions sur la production du riz paddy en Côte d'Ivoire. *Revue Marocaine des Sciences Agronomiques et Vétérinaires*, **9**, 307-316.

[3] Bakker, W. (1975) Rice Yellow Mottle Virus. In: Harrison, B.D. and Murant, A.F., Eds., *CMI/AAB Description of Plant Viruses* (Vol. 149), Commonwealth Mycolog-

ical Institute/Association of Applied Biologist, Wellesbourne, 1-4.

[4] Abo, M.E. (1998) The Mode of Transmission of Rice Yellow Mottle Sobemovirus. Ph.D. Thesis, Ahmadu Bello University, Zaria.

[5] Abo, M.E., Alegbejo, M.D., Sy, A.A. and Misari, S.M. (2000) Overview of the Mode of Transmission, Host Plants and Methods of Detection of *Rice yellow mottle virus*. *Journal of Sustainable Agriculture*, **17**, 19-35. https://doi.org/10.1300/J064v17n01_04

[6] Banwo, O.O., Makundi, R.H., Abdallah, R.S. and Mbapilla, J.C. (2001) Identification of Vectors of *Rice yellow mottle virus* in Tanzania. *Archives of Phytopathology and Plant Protection*, **33**, 395-403. https://doi.org/10.1080/03235400109383361

[7] Sarra, S., Oevering, P., Guindo, S. and Peters, D. (2004) Wind-Mediated Spread of *Rice yellow mottle virus* (RYMV) in Irrigated Rice Crops. *Plant Pathology*, **53**, 148-153. https://doi.org/10.1111/j.0032-0862.2004.00981.x

[8] Lett, J.M. (1997) Approche histopathologique de la résistance du riz (*Oryza sativa*) au virus de la panachure jaune du riz (RYMV). Rapport de DEA. Université Paris VI/Université Paris XI.

[9] Thiémélé Deless, E.F., Kouassi, K.N., Issali, A.E., Albar, L., Aké, S. and Ghesquière, A. (2015) Lutte contre la panachure jaune du riz: Identification de sources de résistance chez le riz africain O. Glaberrima. Fiche technique, WAAPP/PPAAO/CNRA. http://www.waapp-ppaao.org/sites/default/files/lutte_contre_la_panachure_jaune_du_riz_identification_de_sources_de_resistance_chez_le_riz_africain_1.pdf

[10] Raymundo, S.A. and Buddenhagen, I.W. (1976) A Rice Disease in West Africa. *International Rice Commission Newsletter*, **25**, 58.

[11] Awoderu, V.A. (1991) The *Rice yellow mottle virus* Situation in West Africa. *Journal of Basic Microbiology*, **31**, 91-99. https://doi.org/10.1002/jobm.3620310204

[12] N'Guessan, P., Pinel, A., Sy, A., Ghesquière, A. and Fargette, D. (2001) Distribution, Pathogenicity and Interactions of Two Strains of *Rice yellow mottle virus* in Forested and Savanna Zones of West Africa. *Plant Disease*, **85**, 59-64. https://doi.org/10.1094/PDIS.2001.85.1.59

[13] Kashyap, B. and Kumar, R. (2021) Sensing Methodologies in Agriculture for Monitoring Biotic Stress in Plants Due to Pathogens and Pests. *Inventions*, **6**, Article 29. https://doi.org/10.3390/inventions6020029

[14] Fernández, C.I., Leblon, B., Haddadi, A., Wang, K. and Wang, J. (2020) Potato Late Blight Detection at the Leaf and Canopy Levels Based in the Red and Red-Edge Spectral Regions. *Remote Sensing*, **12**, Article 1292. https://doi.org/10.3390/rs12081292

[15] Moshou, D., Pantazi, X.E., Kateris, D. and Gravalos, I. (2014) Water Stress Detection Based on Optical Multisensor Fusion with a Least Squares Support Vector Machine Classifier. *Biosystems Engineering*, **117**, 15-22. https://doi.org/10.1016/j.biosystemseng.2013.07.008

[16] Herrmann, I., Vosberg, S.K., Ravindran, P., Singh, A., Chang, H.X., Chilvers, M.I. and Townsend, P.A. (2018) Leaf and Canopy Level Detection of Fusarium Virguliforme (sudden Death Syndrome) in Soybean. *Remote Sensing*, **10**, Article 426. https://doi.org/10.3390/rs10030426

[17] Tian, L., Xue, B., Wang, Z., Li, D., Yao, X., Cao, Q. and Cheng, T. (2021) Spectroscopic Detection of Rice Leaf Blast Infection from Asymptomatic to Mild Stages with Integrated Machine Learning and Feature Selection. *Remote Sensing of Environment*, **257**, Article ID: 112350. https://doi.org/10.1016/j.rse.2021.112350

[18] Traoré, V.S.E., Néya, B.J., Camara, M., Gracen, V., Offei, S.K. and Traoré, O. (2015) Perception and Impact of *Rice yellow mottle disease* on Rice Yields in Burkina Faso. *Agricultural Sciences*, **6**, 943-952. https://doi.org/10.4236/as.2015.69091

[19] Guinagui, N., Sorho, F., Souleymane, S., Koné, B. and Koné, D. (2019) Effect of *Rice yellow mottle virus*, Sobemovirus on the Contents of N P K Ca and Mg in Leaves of Infected Rice. *Annual Research & Review in Biology*, **30**, 1-10. https://doi.org/10.9734/ARRB/2018/46625

[20] Soro, A.P., Zoro-Diama, E.G., Diomandé, K.S., Bany, G.E., Bisseyou, Y.B.M. and Adohi-Krou, A.V. (2016) Characterization of Water and Nitrogen Stress of Maize by Laser Induced Fluorescence. *Applied Physics Research*, **8**, 64-72. https://doi.org/10.5539/apr.v8n4p64

[21] Zoro-Diama, E.G., Soro, A.P., Diomandé, K.S., Dian, K., Kamate, A. and Adohi-Krou, A.V. (2017) Water Deficiency Detection of Hevea brasiliensis Clones by Laser Induced Fluorescence. *Applied Physics Research*, **9**, 36-41. https://doi.org/10.5539/apr.v9n5p36

[22] Methy, M., Lacaze, B. and Olioso, A. (1991) Prospects and Limits of Fluorescence for Remote Sensing of the Water Status of a Plant Cover: Case of a Soybean Crop. *International Journal of Remote Sensing*, **12**, 223-230. https://doi.org/10.1080/01431169108929648

[23] Dobrowski, S.Z., Pushnik, J.C., Zarco-Tejada, P.J. and Ustin, S.L. (2005) Simple Reflectance Indices Track Heat and Water Stress-Induced Changes in Steady-State Chlorophyll Fluorescence at the Canopy Scale. *Remote Sensing of Environment*, **97**, 403-414. https://doi.org/10.1016/j.rse.2005.05.006

[24] Sun, P., Grignetti, A., Liu, S., Casacchia, R., Salvatori, R., Pietrini, F., Loreto, F. and Centritto, M. (2008) Associated Changes in Physiological Parameters and Spectral Reflectance Indices in Olive (*Olea europaea* L.) Leaves in Response to Different Levels of Water Stress. *International Journal of Remote Sensing*, **29**, 1725-1743. https://doi.org/10.1080/01431160701373754

[25] Gamon, J.A., Penuelas, J. and Field, C.B. (1992) A Narrow-Waveband Spectral Index That Tracks Diurnal Changes in Photosynthetic Efficiency. *Remote Sensing of Environment*, **41**, 35-44. https://doi.org/10.1016/0034-4257(92)90059-S

[26] Rouse, J.W., Haas, R.H., Schell, J.A. and Deering, D.W. (1974) Monitoring Vegetation Systems in the Great Plains with ERTS. *NASA Special Publication*, **351**, 309-317.

[27] Peñuelas, J., Filella, I. and Gamon, J.A. (1995) Assessment of Photosynthetic Radiation-Use Efficiency with Spectral Reflectance. *New Phytologist*, **131**, 291-296. https://doi.org/10.1111/j.1469-8137.1995.tb03064.x

[28] Peñuelas, J., Gamon, J.A., Fredeen, A.L., Merino, J. and Field, C.B. (1994) Reflectance Indices Associated with Physiological Changes in Nitrogen-and Water-Limited Sunflower Leaves. *Remote Sensing of Environment*, **48**, 135-146. https://doi.org/10.1016/0034-4257(94)90136-8

[29] Guyot, G., Baret, F. and Major, D.J. (1988) High Spectral Resolution: Determination of Spectral Shifts between the Red and Infrared. *International Archives of Photogrammetry and Remote Sensing*, **11**, 750-760.

[30] Haboudane, D., Miller, J.R., Tremblay, N., Zarco-Tejada, P.J. and Dextraze, L. (2002) Integrated Narrow-Band Vegetation Indices for Prediction of Crop Chlorophyll Content for Application to Precision Agriculture. *Remote Sensing of Environment*, **81**, 416-426. https://doi.org/10.1016/S0034-4257(02)00018-4

[31] Savitzky, A. and Golay, M.J. (1964) Smoothing and Differentiation of Data by Sim-

plified Least Squares Procedures. *Analytical Chemistry*, **36**, 1627-1639. https://doi.org/10.1021/ac60214a047

[32] Isaksson, T. and Næs, T. (1988) The Effect of Multiplicative Scatter Correction (MSC) and Linearity Improvement in NIR Spectroscopy. *Applied Spectroscopy*, **42**, 1273-1284. https://doi.org/10.1366/0003702884429869

[33] Cortes, C. and Vapnik, V. (1995) Support-Vector Networks. *Machine Learning*, **20**, 273-297. https://doi.org/10.1007/BF00994018

[34] Ballabio, D. and Consonni, V. (2013) Classification Tools in Chemistry. Part 1: Linear Models. PLS-DA. *Analytical Methods*, **5**, 3790-3798. https://doi.org/10.1039/c3ay40582f

[35] Shrestha, S., Deleuran, L.C. and Gislum, R. (2016) Classification of Different Tomato Seed Cultivars by Multispectral Visible-Near Infrared Spectroscopy and Chemometrics. *Journal of Spectral Imaging*, **5**, Article ID: a1. https://doi.org/10.1255/jsi.2016.a1

[36] Römer, C., Bürling, K., Hunsche, M., Rumpf T., Noga, G. and Plümer, L. (2011) Robust Fitting of Fluorescence Spectra for Pre-Symptomatic Wheat Leaf Rust Detection with Support Vector Machines. *Computers and Electronics in Agriculture*, **79**, 180-188. https://doi.org/10.1016/j.compag.2011.09.011